HIGH FRAME RATE ULTRASONIC IMAGING OF ARTERIES FOR DETAILED ANALYSES OF DYNAMICS

HIDEYUKI HASEGAWA[1)2)] AND HIROSHI KANAI[2)1)]

1) Graduate School of Biomedical Engineering, Tohoku University, 6-6-05 Aramaki-aza-Aoba, Aoba-ku, Sendai 980-8579, Japan

2) Graduate School of Engineering, Tohoku University, 6-6-05 Aramaki-aza-Aoba, Aoba-ku, Sendai 980-8579, Japan

Mechanical properties of the arterial walls are significantly altered by atherosclerosis, and various studies have been recently conducted to measure the regional elastic properties (radial strain) of the arterial wall. We have developed a phase-sensitive correlation-based method, namely, the phased-tracking method, to measure the regional radial strain. On the other hand, the measurement of blood flow is an important practical routine in the diagnosis of atherosclerosis. It would be useful if the regional strain of the arterial wall as well as blood flow could be assessed simultaneously. Such measurement would require a high frame rate of several kilohertz. In this study, acquisition of ultrasonic RF echoes at a high frame rate (about 3500 Hz) was achieved using parallel beamforming, in which plane waves were transmitted only three times and receive beamforming created 24 beams for each transmit beam. The accuracy in measurement of the minute radial strain was evaluated by a basic experiment using a cylindrical phantom. The error of the measured strain from the theoretical strain profile and its standard deviation were 4.8% and 9.5%, respectively. Furthermore, the radial strain of a carotid arterial wall and blood flow were simultaneously imaged *in vivo*.

1. Introduction

Mechanical properties of the arterial walls are significantly changed by atherosclerosis, and various studies have been recently conducted to measure the regional elastic properties (radial strain) of the arterial wall [1-3]. We have developed a phase-sensitive correlation-based method, namely, the phased-tracking method, to measure the regional radial strain. On the other hand, the measurement of blood flow is an important practical routine in the diagnosis of atherosclerosis. It would be useful if the regional strain of the arterial wall and blood flow could be assessed simultaneously. Such measurement would require a high frame rate of several kilohertz. In this study, a high frame rate acquisition of ultrasonic RF echoes (about 3500 Hz) was achieved using parallel beam forming [4]. The accuracy in measurement of the minute radial strain was

evaluated by a basic experiment using a cylindrical phantom. Furthermore, the radial strain of a carotid arterial wall and blood flow were simultaneously imaged *in vivo*.

2. Principles

2.1. *Parallel Beamforming*

In conventional linear scanning, both transmit and receive beamforming are performed. Therefore, the frame rate, f_{FR}, is determined by dividing the pulse repetition frequency (PRF), f_{PRF}, by the number of beams, N_{bm}. Typically, frame rate f_{FR} is about 140 Hz when f_{PRF} = 10000 Hz and N_{bm} = 72.

On the other hand, only receive beamforming is performed in parallel beamforming. Many beams are created by receive beamforming for each transmission of a wide beam. For example, a f_{FR} of about 3300 Hz can be achieved when f_{PRF} = 10000 Hz and the number of transmissions, N_{tr}, is 3. Parallel beamforming achieves a high frame rate at the expense of the spatial resolution because transmit beamforming is not performed.

In this study, a plane wave was transmitted using a commercial diagnostic system (α-10, Aloka, Tokyo, Japan) equipped with N_t = 96 elements of a linear array probe, and RF echoes were received by the same 96 elements. Figure 1 shows an illustration of one transmit-receive procedure. One receiving beam was formed using the RF signals received by N_e = 72 of the 96 elements. Therefore, (N_t − N_e) = 24 receiving beams could be formed for each transmission.

The number of transmissions, N_{tr}, was set at 3, and the element number, $\{n_i\}$, used for i-th transmission (i = 0, 1, ..., N_{tr}) is expressed as follows:

$$n_i = (N_t - N_e) \cdot i + j \qquad (j = 0, 1, 2, \dots, N_t). \tag{1}$$

By performing receive beamforming for each of the three transmissions, (N_t − N_e)·N_{tr} = 72 receiving beams were created. In the receive beamforming, focusing was performed with respect to each sampled point in the scanned region. The f_{PRF} was set at 10416 Hz (observable depth: 74 mm), and a f_{FR} of 3472 Hz was achieved. In the present study, the RF signal received by each of the 96 elements was acquired at a sampling frequency of 40 MHz for off-line processing (receive beamforming, calculations of strain and blood flow).

In this study, the imaging plane and the surface of the linear array probe were parallel to the arterial longitudinal direction. Under such condition, the receiving beam at an angle, φ (in Fig. 1), of 90 degrees coincided with the arterial radial direction. Therefore, receiving beams at φ = 90 degrees were

formed to estimate the radial strain of the arterial wall. For imaging of blood flow, receiving beams at φ = 85 and 95 degrees were formed. As shown in Fig. 2, these beamformed RF signals were combined for simultaneous imaging of the radial strain and blood flow. Images of the radial strain of the arterial wall and blood flow in the shadowed region in the right-hand side of Fig. 2 were obtained.

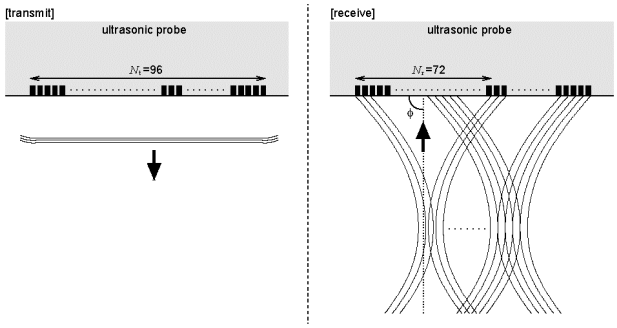

Figure 1.Illustration of one transmit-receive procedure in parallel beamforming.

The beamformed RF signals at φ = 90 degrees were processed as described in [6] to estimate the radial strain. For imaging of blood flow, a standard double delay line canceler was used for high-pass filtering of the beamformed RF signals at φ = 85 and 95 degrees. The power of the high-pass filtered RF signals was estimated and displayed based on the conventional power Doppler technique.

2.2. *Estimation of Two-dimensional Motion of the Arterial Wall*

To obtain complex signals $h(x, z; n)$ (x and z: lateral and axial positions, n: frame number) whose phase relates to the lateral fluctuation of received echoes, the Hilbert transform was applied to envelope signals $\{s(x, z; n)\}$ of RF echoes with respect to the lateral position x as follows:

$$h(x, z; n) = \mathrm{HT}_x[s(x, z; n)], \tag{2}$$

where $\mathrm{HT}_x[\cdot]$ shows the Hilbert transform with respect to x.

Using the complex signal $h(x, z; n)$, the correlation function $R_{(x,z),n}(\tau)$ is evaluated at two different lags, $\tau = \tau_{x1}$ and τ_{x2}, as follows:

$$R_{(x,z),n}(\tau) = \sum_{(x,z)\in R_p} h^*(x, z; n) \cdot h(x + \tau, z; n + 1), \tag{3}$$

where lags τ_{x1} and τ_{x2} were set at 0 and Δx (lateral spacing of scan lines), respectively, and $*$ represents complex conjugate.

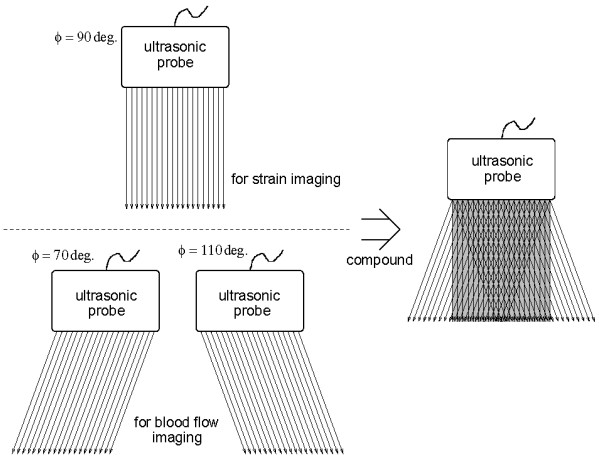

Figure 2. (a) Original elasticity distribution of the tissue. (b) Ascending sequence of the elastic modulus in an elasticity distribution. (c) Normal distribution whose number of boxes depends on the number of data points of (a).

The difference in phases arg[$R_{(x,z),n}(\tau_{x1})$] and arg[$R_{(x,z),n}(\tau_{x2})$] shows that the magnitude of the phase shift caused by the lateral displacement corresponds to Δx (in this case, the lateral displacement is artificially induced by setting the lag in eq. (3) to be τ_{x1} and τ_{x2}). Therefore, the lateral displacement $u_x(x, z; n)$ can be estimated as follows:

$$u_x(x,z;n) = \frac{\Delta x \cdot \angle R_{(x,z),n}(0)}{\angle\left(R^*_{(x,z),n}(0) \cdot R_{(x,z),n}(\Delta x)\right)}. \quad (4)$$

2.3. *Directional Flow Estimation Using Gradient-Based Optical Flow*

Let us define the brightness of a point P(x, z) (x and z: lateral and axial positions) by $I(x, z; t)$ at time t (corresponding to frame n), and point P(x, z) moves to P'($x + u_x$, $z + u_z$) during a short period δt. By assuming that the echo pattern $\{I(x, z; t)\}$ does not change (there is only translation) during a short period δt, the following relationship will be maintained.

$$I(x,z;t) = I(x + u_x, z + u_z; t + \delta t). \quad (5)$$

By applying the Taylor expansion to eq. (5) and neglecting higher-order terms, eq. (6) is obtained as follows:

$$v_x \frac{\partial I}{\partial x} + v_z \frac{\partial I}{\partial z} + \frac{\partial I}{\partial t} = 0, \quad (6)$$

where v_x and v_z are the lateral and axial velocities, respectively.

By setting a region of interest R_p around point P(x, z), mean squared error α expressed by eq. (7) is evaluated as follows:

$$\alpha = \sum_{(x,z)\in R_p} w_{x,z} \left(v_x \frac{\partial I}{\partial x} + v_z \frac{\partial I}{\partial z} + \frac{\partial I}{\partial t}\right)^2, \quad (7)$$

where $w_{x,z}$ is the weight which is defined as the mean of envelope-detected signals in R_p.

By minimizing α in eq. (7) based on the least squares procedure, two-dimensional velocities v_x and v_z at point P(x, z) at t (= frame n) are estimated.

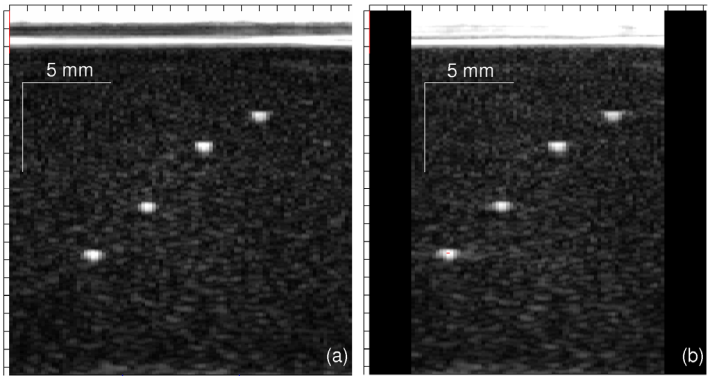

Figure 3. B-mode images of fine wires embedded in agar. (a) Conventional linear scanning. (b) Parallel beamforming. (c) Amplitude profiles along the cyan lines in (a) and (b), which are normalized by the maximum amplitudes of the respective profiles.

3. Basic Experimental Results

3.1. *Comparison of Spatial Resolutions of Conventional Linear Scanning and Parallel Beamforming*

Nylon wires (0.1 mm in diameter) embedded in agar (403GS, Gammex, Inc., Middleton, WI, USA) were imaged to investigate the spatial resolution in parallel beamforming.

Figures 3(a) and 3(b) show B-mode images obtained by conventional linear scanning and parallel beamforming, respectively. Clear images of the four wires were obtained. In the measurement by conventional linear scanning, RF signals focused in real time were acquired at a sampling frequency of 40 MHz.

As shown by these results, the spatial resolution was slightly degraded, but parallel beamforming achieved a much higher frame rate (3472 Hz).

3.2. *Measurements of the Cylindrical Phantom for Evaluation of Accuracy in Strain Estimation*

In basic experiments for evaluation of the accuracy of strain estimation, a cylindrical phantom made of silicone rubber was measured by ultrasound. The outer and inner diameters were 10 and 8 mm, respectively. The phantom

contained 5% carbon powder (by weight) to obtain sufficient scattering from inside the wall.

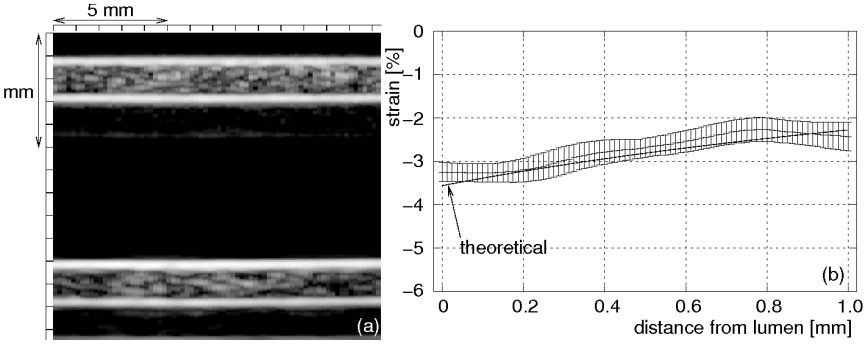

Figure 4. (a) B-mode image of the phantom in the longitudinal plane. (b) Radial strains plotted as a function of the distance from the luminal boundary of the posterior wall. Plots and vertical bars are means and standard deviations for 72 ultrasonic beams.

Change in pressure inside the phantom was induced by circulating a fluid using a flow pump. The change in internal pressure was measured by a pressure sensor (NEC, Tokyo, 9E02-P16). The applied pulse pressure was 48 mmHg.

To measure the elastic moduli of silicone rubber for the calculation of the theoretical strain profile, pressure-diameter testing was conducted. In that testing, the change in external diameter of the phantom was measured with a laser line gauge (KEYENCE, Osaka, VG-035).

Figure 4(a) shows a longitudinal B-mode image of the phantom obtained by parallel beamforming. In Fig. 4(a), angles φ of the receiving beams were 90 degrees. The radial strain distribution in the posterior wall was then estimated by the method described in [6] using the phases of RF echoes. In Fig. 4(b), the estimated radial strains are plotted as a function of the distance from the luminal boundary of the posterior wall (in the directions of the ultrasonic beams). Plots and vertical bars show the mean and standard deviation, respectively, at each radial position r, which were obtained by the individual strain distributions along 72 ultrasonic beams. The solid curve in Fig. 4(b) shows the theoretical radial strain $\varepsilon_{r,r}$ of a homogeneous tube at each radial position r, which was obtained using the elastic modulus E measured by different pressure-diameter testing and the measured internal pressure. The estimated strain distribution agrees well with the theoretical strain profile. Mean error e_{mean} and standard deviation SD_{mean} were 4.8% and 9.5%, respectively.

4. *In Vivo* Experimental Results

4.1. *Simultaneous Imaging of Artery-Wall Radial Strain and Blood Flow*

The right common carotid artery of a 33-year-old male was measured *in vivo*. The beamformed RF signals were envelope-detected and converted into brightness. The envelope-detected signals (instantaneous amplitude) were normalized by their maximum value among all frames. Let us define the normalized envelope by $G_p(j, l; k)$, where j, l, and k define depth, beam number, and frame number, respectively. The radial strain of the posterior wall was estimated by applying the same procedure as in [6] to the beamformed RF signals at φ = 90 degrees.

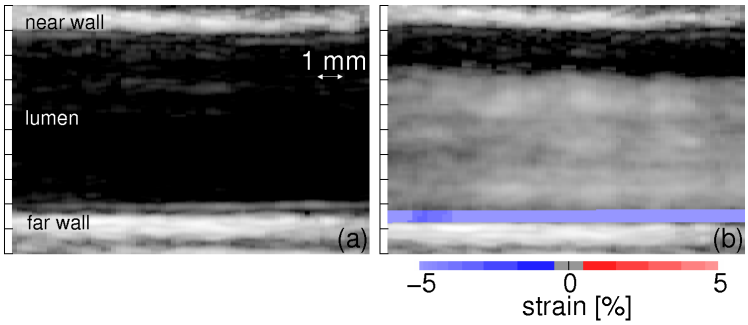

Figure 5. Ultrasonic images of the carotid artery of a 33-year-old male obtained at (a) the time of R-wave and (b) 0.15 s after R-wave.

Blood flow was imaged using ultrasonic beams formed with angles φ of 85 and 95 degrees. Obliquely beamformed RF signals were high-pass filtered using a standard double delay line canceler. The powers of the high-pass filtered RF signals were estimated by the conventional power Doppler technique. The number of frames used for calculation of the average power was 64. The roots of the estimated average power were normalized by their maximum among all frames. Let us define the normalized roots of power by $G_{85}(j, l; k)$ and $G_{95}(j, l; k)$ for beam angles φ of 85 and 95 degrees, respectively. The regions scanned by beams at these angles overlap. The normalized root of power, $G_o(j, l; k)$, for obliquely formed beams is defined as follows:

$$G_o(j,l;k) = \begin{cases} G_{85}(j,l;k) \text{ or } G_{95}(j,l;k) & (beams\ do\ not\ overlap), \\ \frac{G_{85}(j,l;k)+G_{95}(j,l;k)}{2} & (beams\ overlap). \end{cases} \quad (8)$$

Echo amplitude $G(j, l; k)$ at each point (j, l) in the k-th frame was obtained as follows:

$$G(j,l;k) = \alpha G_p(j,l;k) + (1-\alpha)G_o(j,l;k) \qquad (0 \le \alpha \le 1). \tag{9}$$

In this study, α was set at 0.9.

Figure 5(a) and 5(b) show images of $G(j, l; k)$ at the R-wave of the electrocardiogram and 0.15 s after the R-wave. As shown in Fig. 5(b), echoes from blood particles are enhanced when the blood flow velocity is high (at 0.15 s). This result shows that the proposed method successfully imaged blood flow.

4.2. *Estimation of 2D Motion of Arterial Wall*

Complex deformation of atherosclerotic plaque would relate to its vulnerbility. We tried to estimate such complex motion of a carotid atherosclerotic plaque. The red points in Fig. 4 show points of interest set in the posterior wall of the carotid artery. As shown in Fig. 6(b), in cardiac systole, there are stretch and shearing along the arterial longitudinal direction in addition to radial strain. Assessment of such complex motion and deformation would be useful for evaluation of plaque vulnerability.

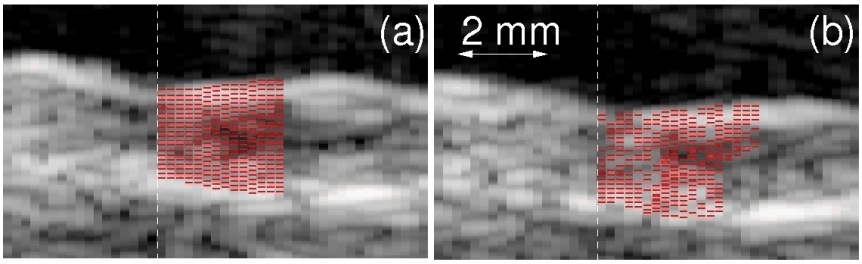

Figure 6. Two-dimensional tracking of points of interest (shown by the red points) in the posterior wall of the carotid artery. At (a) 0 s and (b) 0.21 s after the time of R-wave of electrocardiogram.

4.3. *Directional Flow Velocity Estimation*

Figures 7(a) and 7(b) show blood flow images at two different moments. The time difference is 6.6 ms, and there are 30 other images between them. In Fig. 7(c), estimated velocities are shown by the red lines. As is well known, the magnitude of the estimated velocity decreases near the arterial wall. Although further improvements and quantitative validation are required, this result shows the possiblity of the proposed method for quantitative measurement of blood flow.

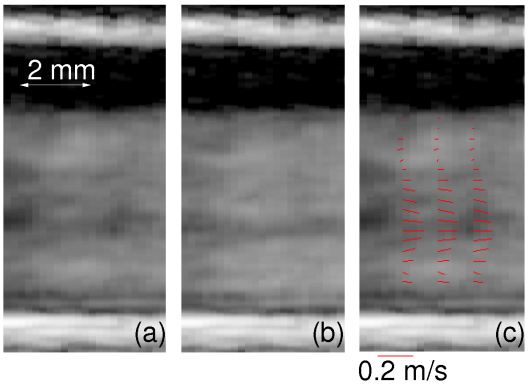

Figure 7. (a) Blood flow image and (b) that 6.6 ms after (a). (c) Flow velocity estimated by gradient-based optical flow.

4.4. *Measurement of Pulse Wave Velocity*

One strategy for assessment of artery-wall elasticity is the measurement of pulse wave velocity. Figure 8 shows the velocities of the carotid arterial wall measured at intervals of 0.2 mm along the arterial longitudinal direction. The velocity waveforms were sampled at 3472 Hz. It was difficult to identify the leading edges of the pulsive velocities. Therefore, transients of the central time of velocity peaks were observed. There was a difference of about 2 ms in the central times during the propagation along a distance of 14.4 mm. The propagation velocity was roughly estimated to be 7 m/s. The proposed high frame rate imaging would be useful for the measurement of regional pulse wave velocity. However, it was difficult to differentiate the change in velocity waveform and the time shift due to propagation in time domain. Frequency domain analysis of velocity waveforms would be useful for the evaluation of the linearity between waveforms and the precise estimation of time delay.

5. Conclusions

In this study, a high frame rate acquisition of RF echoes (3472 Hz) was achieved using parallel beamforming which realizes the simultaneous imaging of artery-wall strain and blood flow. Using the proposed method, the arterial wall strain and blood flow of a carotid artery were successfully imaged *in vivo*. The proposed method would provide useful information on the dynamics of the artery for diagnosis of atherosclerosis.

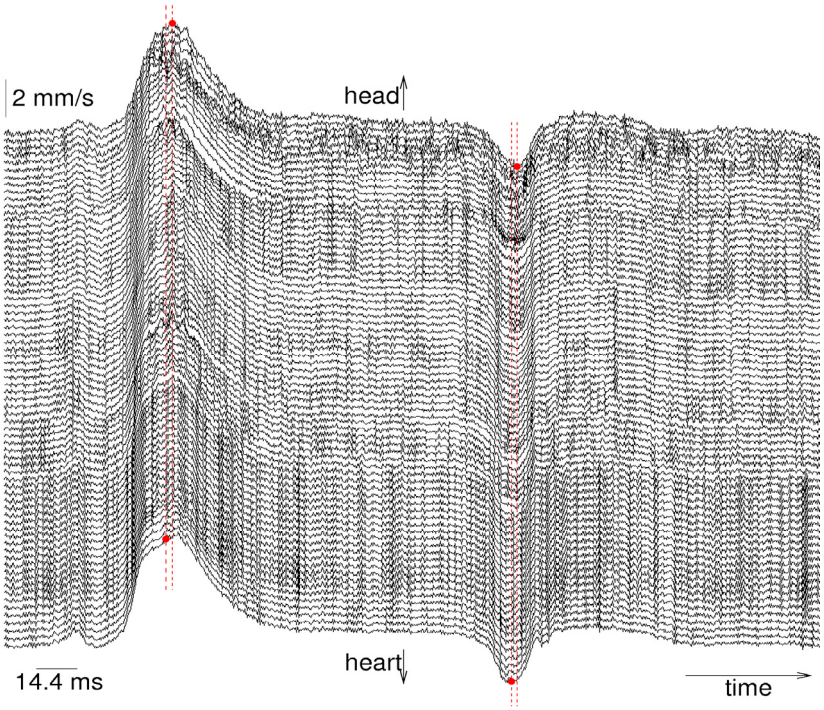

Figure 8. Velocity waveforms of posterior wall measured at intervals of 0.2 mm along the arterial longitudinal direction.

References

1. C. L. de Korte, E. I. Céspedes, A. F. W. van der Steen and C. T. Lanée, Intravascular elasticity imaging using ultrasound: Feasibility studies in phantoms. *Ultrasound Med Biol* **23**, 735-746 (1997).
2. H. Kanai, H. Hasegawa, M. Ichiki, F. Tezuka and Y. Koiwa, Elasticity imaging of atheroma with transcutaneous ultrasound –preliminary study-. *Circulation* **107**, 3018 (2003).
3. R. L. Maurice, J. Ohayon, Y. Fr´etigny, M. Bertrand, G. Soulez and G. Cloutier, Noninvasive vascular elastography: Theoretical frame. *IEEE Trans. Med. Imaging* **23**, 164 (2004).
4. M. Tanter, J. Bercoff, L. Sandrin and M. Fink, Ultrafast compound imaging for 2-D motion vector estimation: Application to transient elastography. *IEEE Trans. Ultrason. Ferroelectr. Freq. Control* **49**, 1363 (2002).
5. H. Hasegawa and H. Kanai, Simultaneous imaging of artery-wall strain and blood flow by high frame rate acquisition of RF Signals. *IEEE Trans. Ultrason. Ferroelectr. Freq. Control* **55**, 2626 (2008).
6. H. Hasegawa and H. Kanai, Modification of the phased-tracking method for reduction of artifacts in estimated artery wall strain. *IEEE Trans. Ultrason. Ferroelectr. Freq. Control* **55**, 1921 (2008).